Electronic Supplementary Material (ESI) for Nanoscale.

Supplementary information

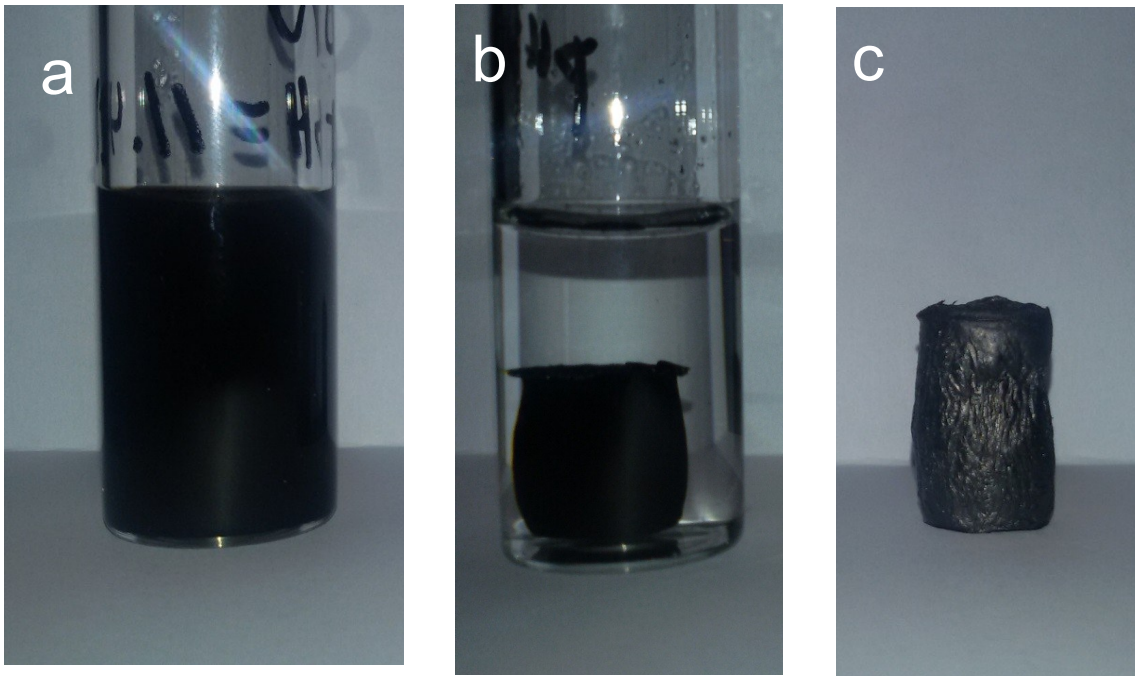

Figure S1. Initial dispersion (a), hydrogel after 2 h of hydrothermal treatment time (b) and aerogel after freeze drying (c)

Textural characterisation by N2 and CO2 physisorption

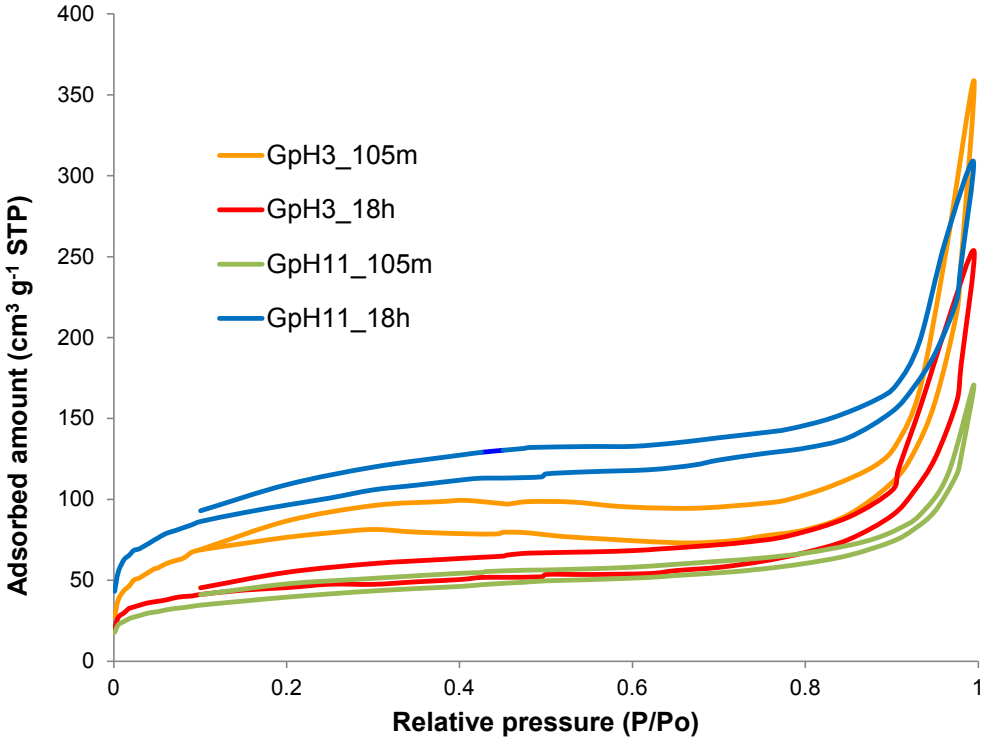

Figure S2. N_2 adsorption isotherms of graphene aerogels prepared under different pH conditions and times

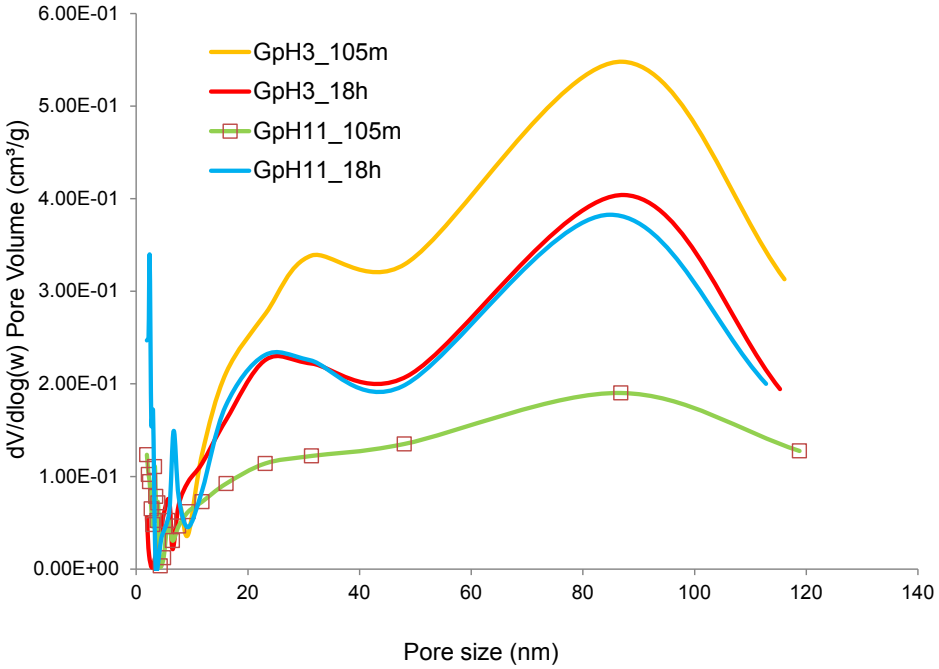

Figure S3. Pore size distribution calculated by the BJH method from the N_2 adsorption branch of the isotherm.

UV spectrophotometry of the reduction hydrothermal process

The dispersions of GO nanosheets before gelation were analyzed by UV-spectrophotometry (Figure 1). The absorbance of GO colloidal dispersions in the 200–250 nm range with the well-pronounced maximum at 230 nm is assigned to various oxygen functional groups such as to conjugated ketones or dienes.[6, 7] For longer durations of hydrothermal treatment, the absorption peak of the GO dispersion at 230 nm gradually redshifts to 260 nm and the absorbance in the 270–350 nm region increases, which is deemed to be due to the increase of conjugated aromatic domains. Moreover, the absorbance of aqueous dispersions in the broad region 230–700 nm increases with time in accordance with the change to a black colour. This indicates that the electronic conjugation level of graphene is chemically controllable while the platelets of partially reduced graphene (rGO) are dispersed before the formation of the hydrogel.

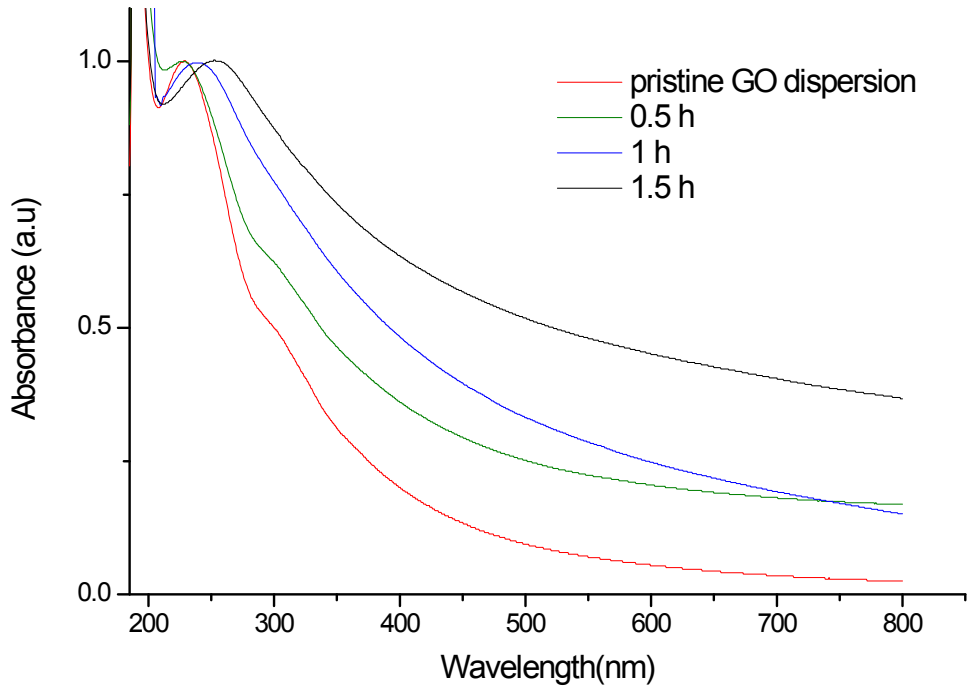

Figure S3. UV–vis spectra of the aqueous solutions of the diluted GO samples after different times of hydrothermal treatment at pH=3.

XPS

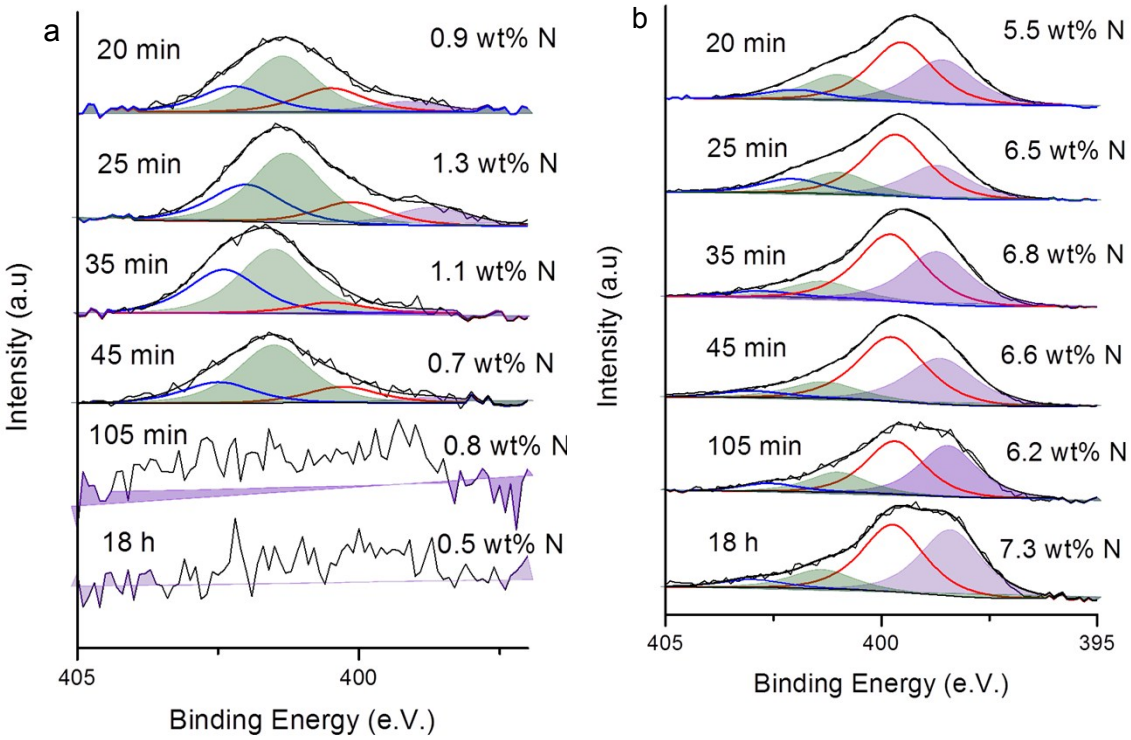

Figure S4. Fitting of XPS N 1s of aerogels after different times prepared under pH=3 (a) and pH=11 (b)

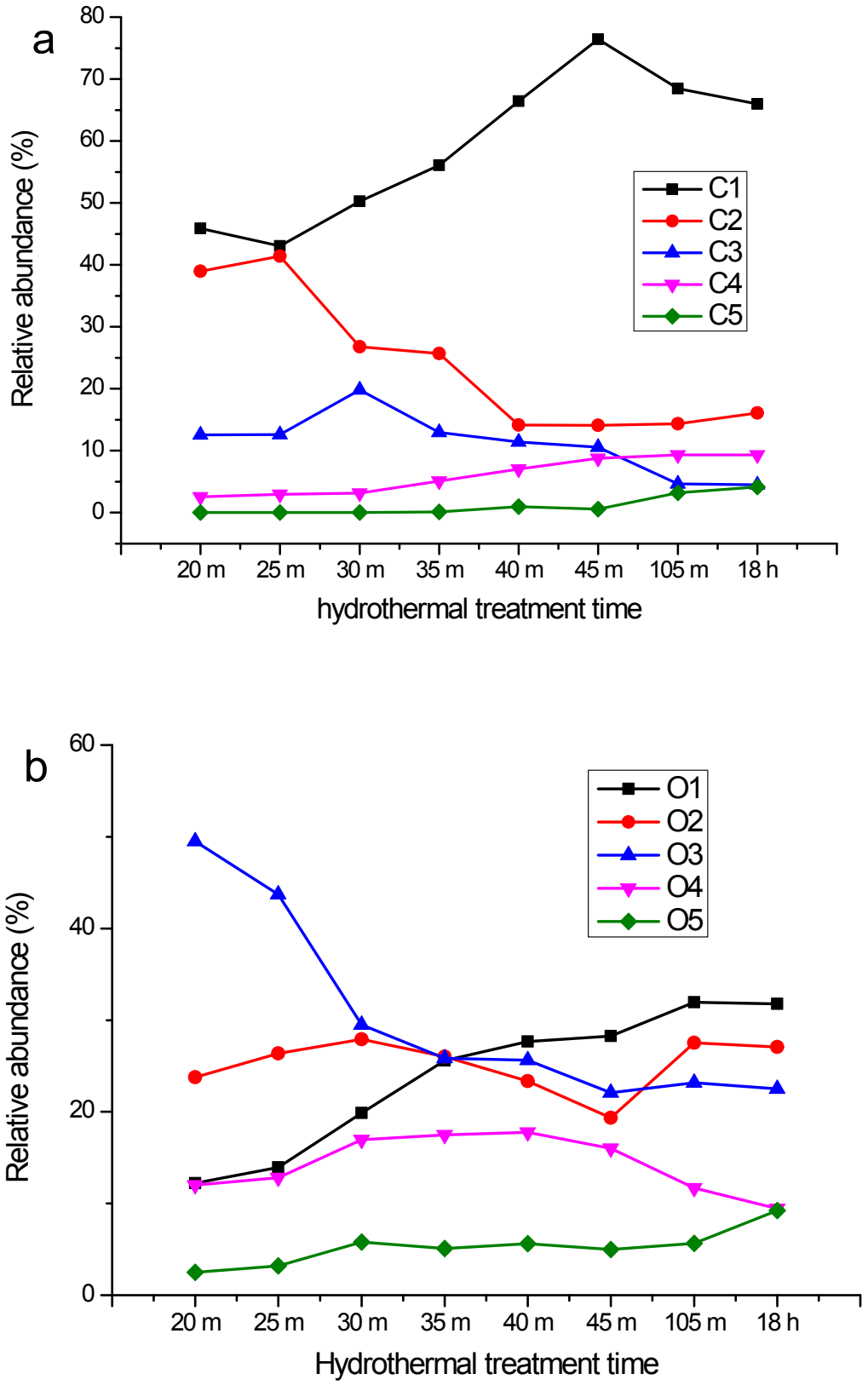

Figure S5. Relative abundance of components of XPS C 1s (a) and O 1s (b) peaks for aerogels prepared at pH=3

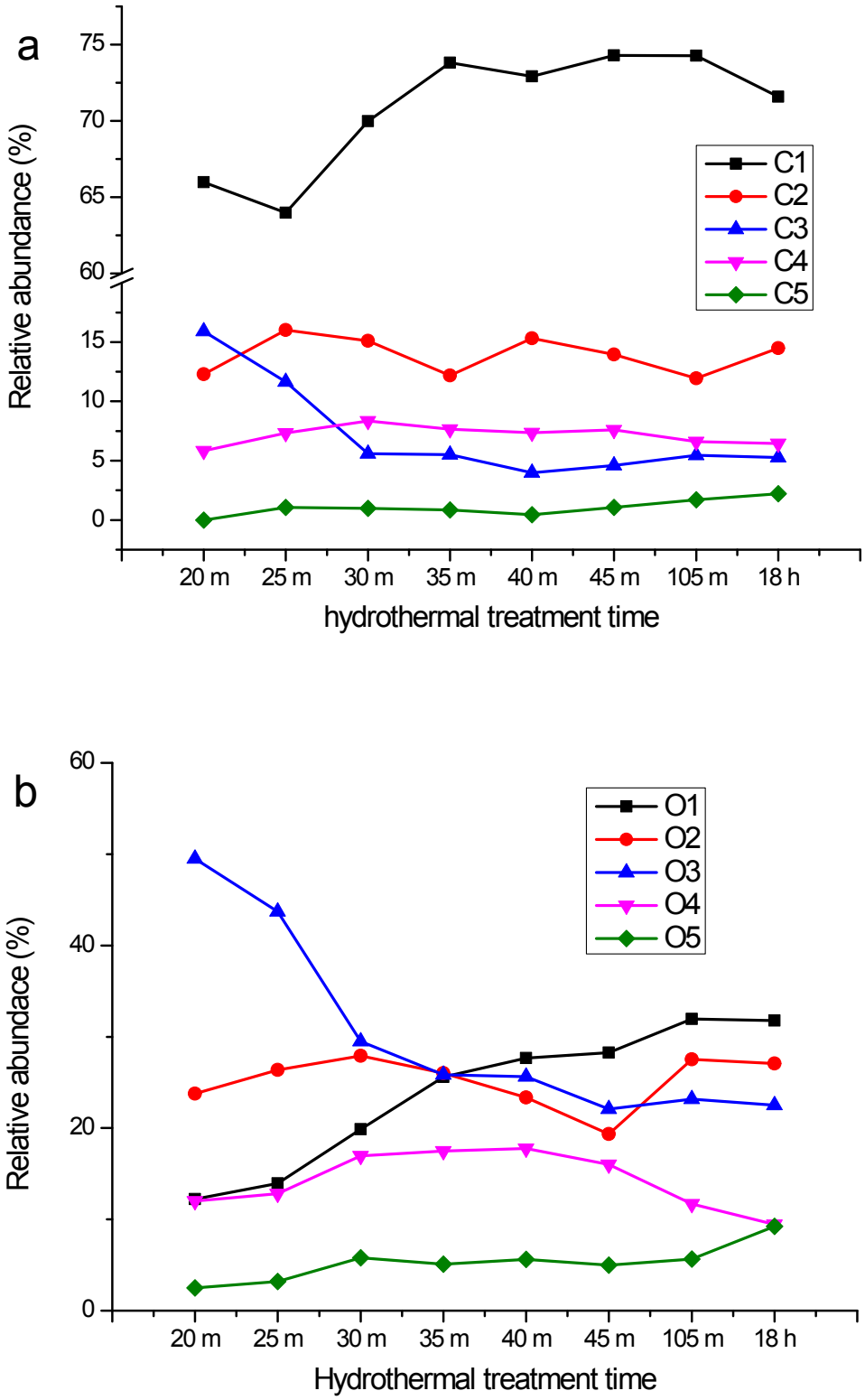

Figure S6. Relative abundance of components of XPS C 1s (a) and O 1s (b) peaks for

aerogels prepared at pH=11

TPD

Surface chemistry was further characterized by temperature programmed desorption (TPD). TPD profile for GO shows a sharp desorption of CO_2, CO at 529 K (Figures S7 b,c). H_2O desorption (Figure S7a) for GO shows also a peak at slightly higher temperature (550 K) and a shoulder that extends for higher temperatures. It was reported that, when GO is treated thermally at 453-493 K, it quickly "pops," expanding its volume for *ca.* 2 orders of magnitude.[8] This is attributed to the release of CO_2 and H_2O intercalated between the graphene oxide nanosheets and decomposition of some oxygenated surface groups. The remaining oxygenated groups evolving at temperatures above 600 K are even less than those for the graphene aerogels.

For graphene aerogels, desorption of H_2O, CO_2 and CO during TPD occurs in a more progressive manner over a broader temperature range, spanning between 400-1200 K for H_2O and CO_2 and between 800-1273 K for CO. The H_2O desorption exhibits a maximum at a higher temperature (650 K) than that found for GO, which can be attributed to intercalated water or chemisorbed water. In the literature, the CO_2 and CO TPD profile has been fitted to several peaks that have been assigned to some specific groups but this entails some ambiguity. However, some general trends have been established:[9-12] (a) carboxyl anhydrides generate both a CO and CO_2 peak around 800-900 K; (b) CO_2 peak results from decomposition of carboxylic acids at low temperatures, or lactones at high temperatures; (c) CO desorption is produced from phenols and semiquinones at lower temperatures than quinones and carbonyls.

The shoulder in CO_2 profile at 630-650 K can be ascribed to carboxylic acids since it coincides with a desorption peak of H_2O. For the aerogels prepared at pH=11, the carboxylic acid and anhydride peaks diminish substantially, phenol peak decrease slightly but the intensity of basic group peaks such as lactones and quinone groups, desorbing CO at high temperature, do not decrease. The amount of total oxygen content, especially the more basic groups desorbing as CO at high temperature, decreased as the time of hydrothermal treatment increased for pH=11 and it stays stable for pH=3 . These findings are in agreement with FTIR characterization.

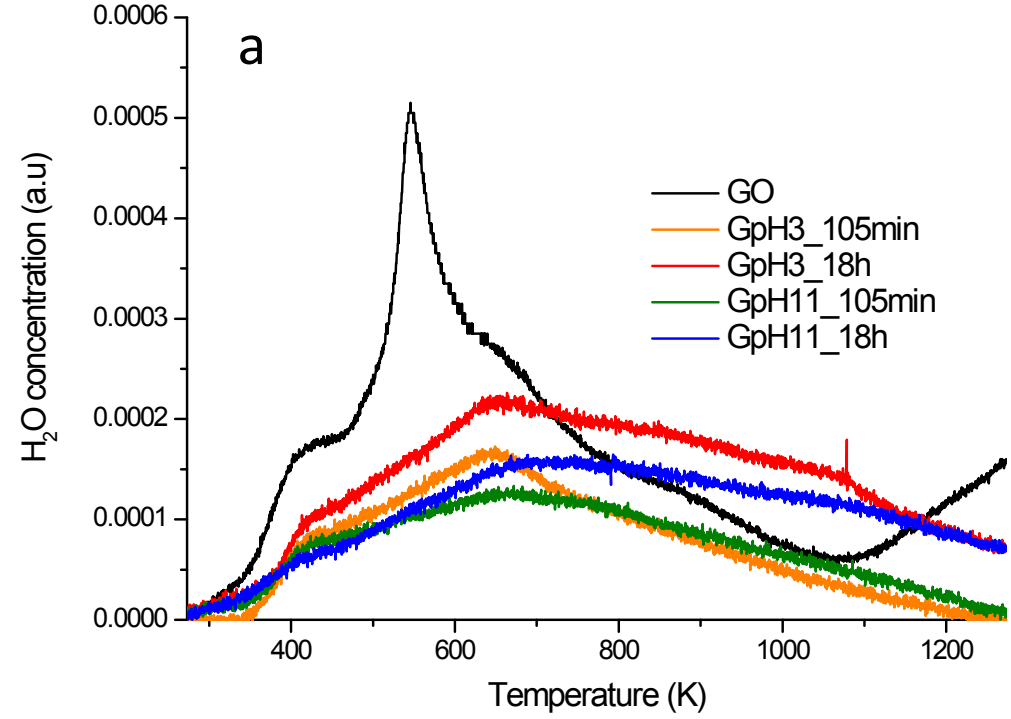
a
0.0006
0.0005
0.0004
0.0003
0.0002
0.0001
0.0000
H2O concentration (a.u)
400
600
800
1000
1200
Temperature (K)
GO
GpH3_105min
GpH3_18h
GpH11_105min
GpH11_18h

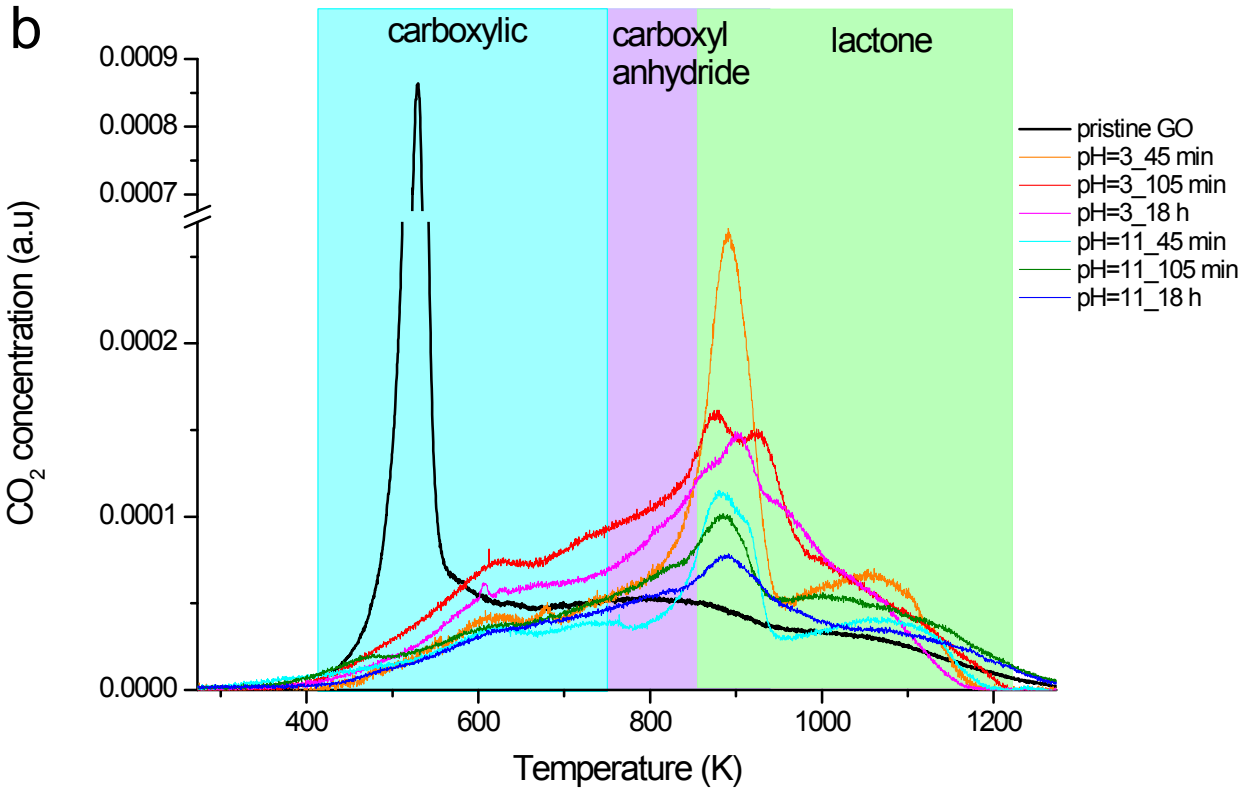
b
carboxylic
carboxyl anhydride
lactone
0.0009
0.0008
0.0007
0.0002
0.0001
0.0000
CO2 concentration (a.u)
400
600
800
1000
1200
Temperature (K)
pristine GO
pH=3_45 min
pH=3_105 min
pH=3_18 h
pH=11_45 min
pH=11_105 min
pH=11_18 h

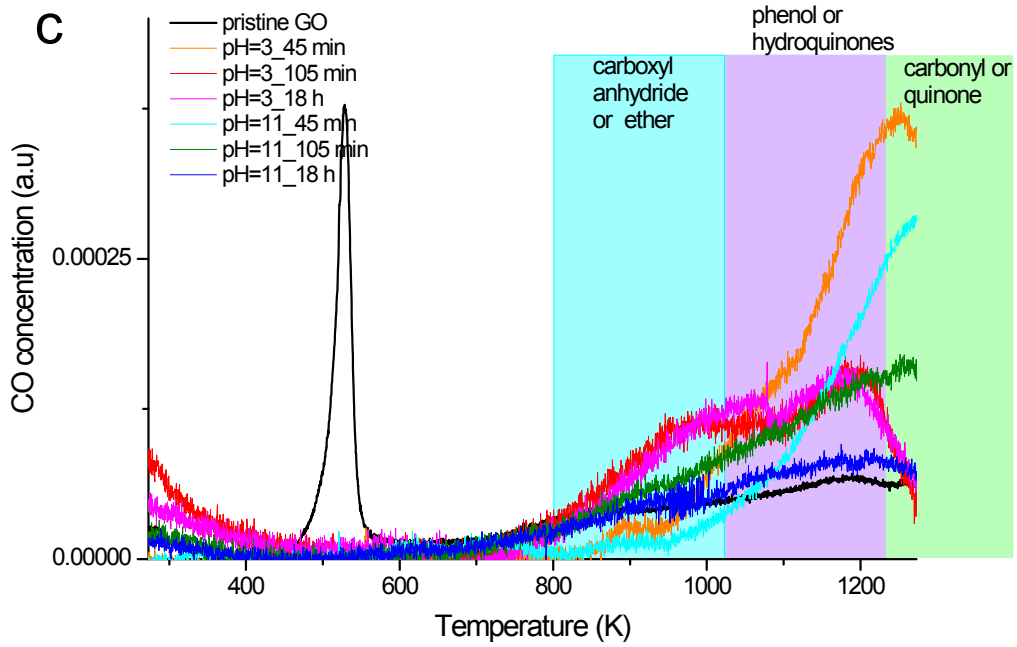

Figure S7. Temperature programmed desorption (TPD) profile of H_2O (a), CO_2 desorption (b) and CO desorption (c) for the different materials such as pristine GO (black trace) and graphene aerogels prepared at different conditions: GpH3_105min (orange trace), GpH3_18h (red trace), GpH11_105min (green trace), GpH11_18h (blue trace).

Table 3. Oxygen content by elemental analysis and quantification of TPD experiments

Elemental analysis			TPD quantification		
	O %	C/O	CO µmol g^{-1}	CO_2 µmol g^{-1}	CO_2/CO
GO	44.4	1.2	1868	4065	2.1
GpH3_105min	18.5	4.4	2309	4393	1.9
GpH3_18h	18.0	4.5	2217	3686	1.7
GpH11_105min	16.8	4.9	2105	2748	1.3
GpH11_18h	11.2	7.9	1427	2175	1.5

Selective absorption of organics

Due to the different liquid density, the tri-phasic system consists of hexane at the top, water at the middle and dichloromethane settled at the bottom. Both organic solvents are red coloured using Sudan III. When introduced in the vial, the aerogel monolith absorbs readily hexane (10 s). Since the aerogel monolith is repelled by water, it is necessary to push it to the bottom with tweezers. When the bottom is reached, it absorbs readily dichloromethane while releasing the air inside as bubbles. It is thus revealed that water hardly penetrates inside the aerogel while the non-polar solvents are selectively absorbed. This was also confirmed by contact angle measurements since the contact angle of a water droplet was 84º and it is slowly adsorbed (Figure S9 and movie 2 of supplementary information) while toluene is absorbed instantaneously rendering the measurement of contact angle elusive (movie 3). The aerogel GpH11_18h was recycled for at least 10 cycles by evaporating the organic solvent at 107 ºC, keeping the absorption capacity and mechanical robustness (Figure S10 supplementary information). In turn, this regeneration method allows the recovery of the organic solvent by distillation.

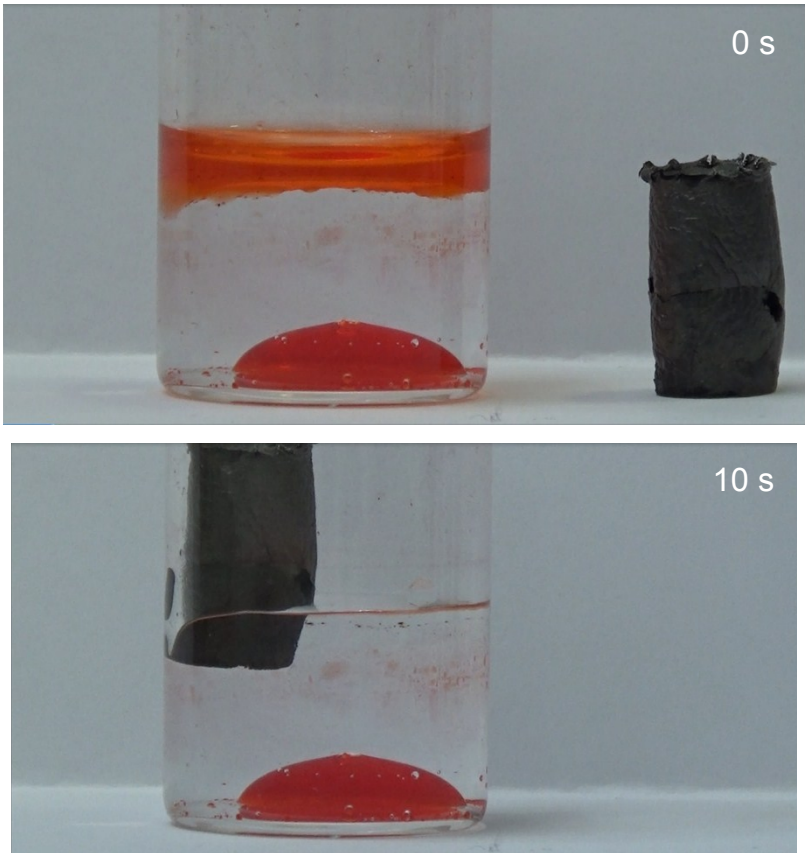

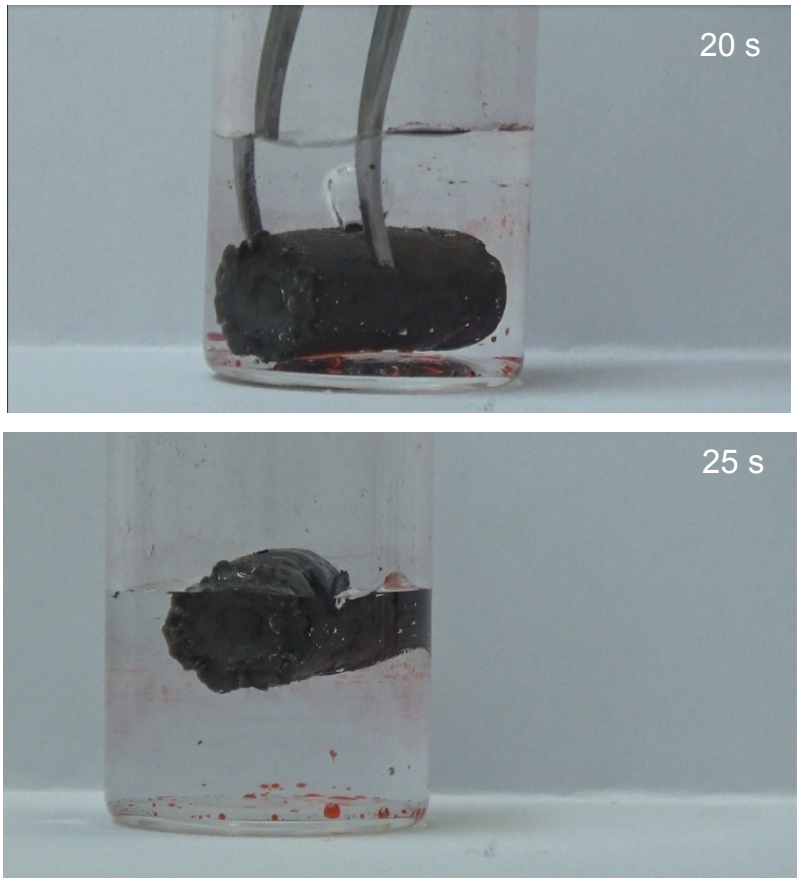

Figure S8. Photograms illustrating the selective absorption of non-polar solvents.

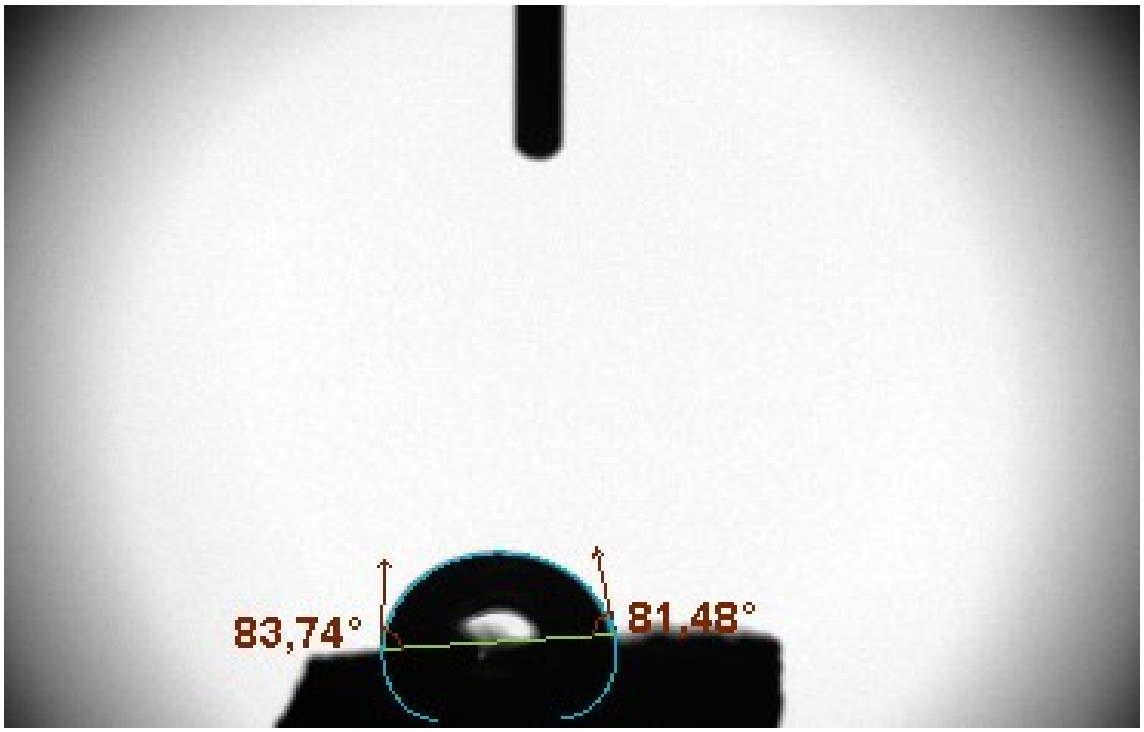

Figure S9. Water contact angle

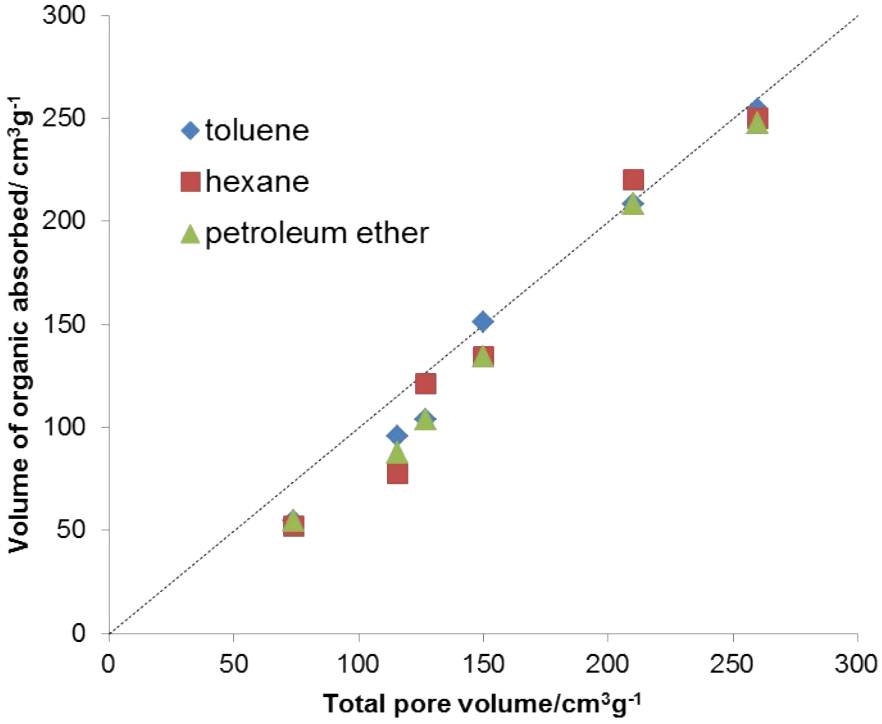

Figure S10. Plot of the volume of organic absorbed versus the total pore volume of the aerogel for the different organics

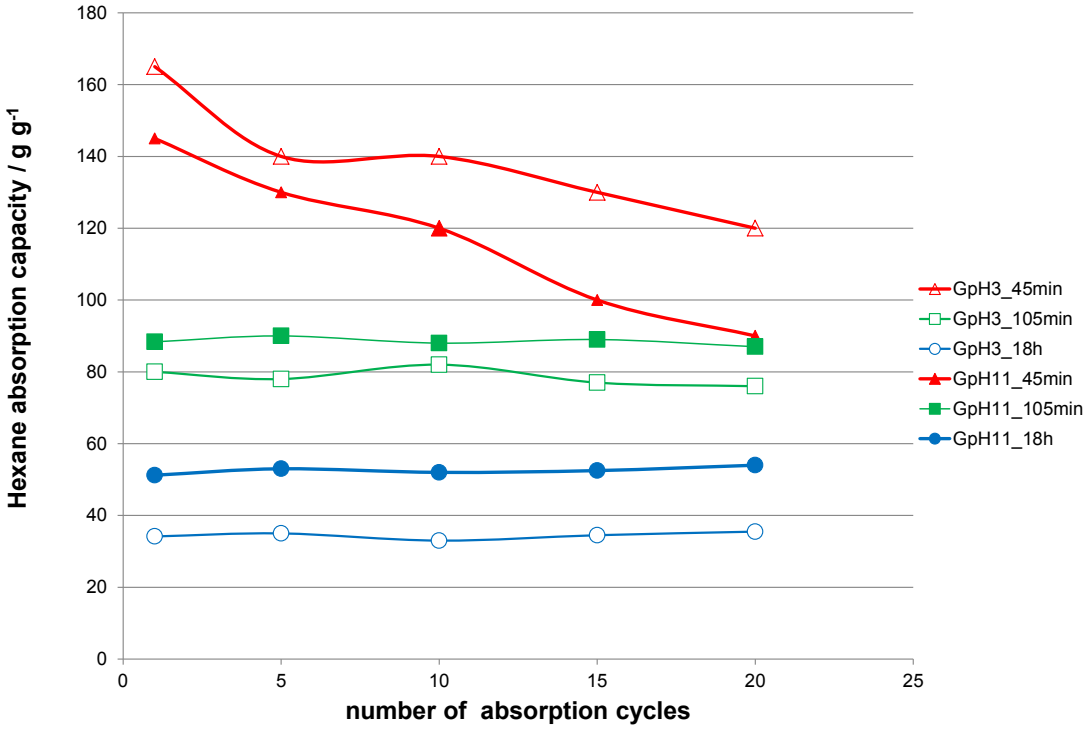

Figure S11. Hexane absorption capacity as a function of number of cycles for 20 cycles of absorption and subsequent distillation of solvent at 107 ºC.

Reference List

1. P. B. Balbuena and K. E. Gubbins, *Fluid Phase Equil.*, 1992, **76**, 21-35.
2. K. S. W. Sing, *Journal*, 1985, **57**, 603.
3. K. Kaneko, *J. Mem. Sci.*, 1994, **96**, 59-89.
4. D. Lozano-Castelló, D. Cazorla-Amorós and A. Linares-Solano, *Carbon*, 2004, **42**, 1233-1242.
5. A. Wahby, J. Silvestre-Albero, A. Sepúlveda-Escribano and F. Rodríguez-Reinoso, *Mic. Mes. Mater.*, 2012, **164**, 280-287.
6. A. Dimiev, D. V. Kosynkin, L. B. Alemany, P. Chaguine and J. M. Tour, *J. Amer. Chem. Soc.*, 2012, **134**, 2815-2822.
7. D. Li, M. B. Muller, S. Gilje, R. B. Kaner and G. G. Wallace, *Nat Nano*, 2008, **3**, 101-105.
8. Y. Gao, X. Chen, J. Zhang, H. Asakura, T. Tanaka, K. Teramura, D. Ma and N. Yan, *Adv. Mater.*, 2015, **27**, 4688-4694.
9. J. L. Figueiredo, M. F. R. Pereira, M. M. A. Freitas and J. J. M. Orfao, *Carbon*, 1999, **37**, 1379-1389.
10. S. Haydar, C. Moreno-Castilla, M. A. Ferro-García, F. Carrasco-Marín, J. Rivera-Utrilla, A. Perrard and J. P. Joly, *Carbon*, 2000, **38**, 1297-1308.
11. Y. Otake and R. G. Jenkins, *Carbon*, 1993, **31**, 109-121.
12. G. S. Szymański, Z. Karpiński, S. Biniak and A. Świątkowski, *Carbon*, 2002, **40**, 2627-2639.